以資料發掘與視覺模型為基礎之電腦輔助超音波肝臟腫瘤之區別診斷(3/3)

Computer Assisted Differential Diagnosis of Hepatic Tumors in Ultrasound Images Based on Data Mining and Vision Models (3/3)

計畫編號：NSC 90－2213－E－002－123－
執行期限：90 年 8 月 1 日至 91 年 7 月 31 日

主持人：　陳中明　國立台灣大學醫學工程學研究所
共同主持人：　許金川　國立台灣大學醫學院內科
盧鴻興　國立交通大學統計研究所

1. Abstract

In the third year, we have developed a new segmentation scheme, which is capable of extracting multiple hepatic tumors simultaneously from an ultrasound image. Moreover, we have combined the segmentation results and the classification scheme to achieve a classification accuracy of 85.78% with leave-one-out cross-validation by using only texture information. As a future study, it is believed that the performance can be further improved by incorporating the characteristics of the boundary vicinity information.

Keywords: Computer assisted diagnosis, Hepatic tumor, Ultrasound image, Image Segmentation, Data Mining

中文摘要

在第三年計畫中，我們發展出可以從超音波影像中同時分割出多個腫瘤的技術，並且結合了分割的結果與分類的技術而達到 85.78%的良惡性腫瘤辨識率。此一結果僅使用了紋路訊息。作為研究的下一個工作，我們相信加入邊緣附近的訊息將可進一步的改良辨識率。

關鍵詞：電腦輔助診斷、肝臟腫瘤、超音波影像、影像分割、資料發掘

2. Introduction

Two essential tasks have been carried out in the third year of this project. The first task was to develop a new segmentation algorithm, which is capable of extracting multiple tumors from an ultrasound image at the same time. It is a very useful technique because it may contain more than one tumor in a clinical ultrasound image. On the other hand, after a tumor was segmented from the liver, a set of features were extracted from the ROI and a multi-layer feed-forward neural network (MFNN) was employed as the classifier to differentiate HCCs from hemangiomas.

For segmenting multiple tumors simultaneously, a new approach, called cell-based region competition, for ultrasound image segmentation was developed. The basic idea of the proposed approach was to decompose the underlying image into cells with similar image property and combine the cells into regions, each of which may comprise more than one cell. Algorithmically, the first step was to apply multi-scale Gaussian filters to remove the speckle noises and preserve edge information. Then, filters, like the Sobel filter, were used to estimate the gradient vectors. With the gradient vectors, an initial segmentation was generated by the watershed transform [1,2]. These initial regions were further combined by the technique of region competition [3,4] based on likelihood ratio tests among cells.

Two categories of features have been utilized to characterize the regional information for the benign and the malignant tumors, namely, the co-occurrence matrix based features and the local variance-to-mean based features.

2. The Cell-based Region Competition

In the proposed cell-based region competition approach, multi-scale Guassian filters are first used to smooth the initial image and preserve the edge information. Sobel filters are then used to generate the gradient map that consists of the absolute values of gradient vectors. Immersion

simulation [1] is used to produce the watershed transform that generates initial cells. Neighboring relationships of initial cells are stored in a neighborhood matrix. Cells are combined into regions and regions may be further split. The merging and splitting are based on the likelihood ratio tests of the original ultrasound images. The neighborhood matrix is updated and merging/splitting iterates until stopping criteria are met.

2.1. Neighborhood Matrix

The initial cells are generated after the watershed transform. When two or more cells are merged, it is called a region. If a region consisting of two cells is split, this region dismissed. To keep tracking the neighboring relationship of these cells and regions as the cell-based split and merge proceeds, a neighborhood matrix is constructed to record the relations among adjacent cells and regions. Let A denote the neighborhood matrix. If cells (or regions) *i* and *j* are next to each other, $a_{ij} = a_{ji} = 1$. Otherwise, $a_{ij} = a_{ji} = 0$. The diagonal entries are set to be zeros, i.e., $a_{ii} = 0$. Thus, the neighborhood matrix is a symmetric matrix with entries of 0 or 1.

2.2. Cell-based Split-and-Merge

Three types of splitting and merging have been considered in this study. These three types are Types Ⅰ, Ⅱ, and Ⅲ, which represent competition between two cells, one cell and one region, as well as one region and one cell in another region, respectively.

2.2.1. Type Ⅰ

Type I split-and-merge is defined as merging two adjacent cells into a new region. Suppose that cells *i* and *j* may be characterized by two probability distributions, e.g., the Rayleigh distributions, with parameters σ_i and σ_j. Then the null and alternative hypotheses are

$$H_0 : \sigma_i = \sigma_j \quad vs. \quad H_1 : \sigma_i \neq \sigma_j .$$

If the null hypothesis is not rejected, cells *i* and *j* are merged into a new region.

2.2.2. Type Ⅱ

Type Ⅱ is defined as merging a cell into a region. Suppose that region *k* and cell *j* have probability distributions with parameters σ_k and σ_j. The hypothesis testings for two cells and one cell and one region are similar. However, there is no new region generated for one cell and one region.

$$H_0 : \sigma_k = \sigma_j \; vs. H_1 : \sigma_k \neq \sigma_j .$$

2.2.3. Type Ⅲ

Suppose cells 1 and 6 in Fig. 1 formed a region, called region 1. Cells 2, 3 and 4 formed a region, labeled as region 2. At some point, cell 4, which is delineated by a dashed boundary, is re-evaluated to check if it is better to split cell 4 from region 2 and merge it into region 1. If cell 4 is split from region 2, the new region 2 would only consist of cells 2 and 3. The parameters of probability distributions in cell 4, new region 2 (of cell 2 and 3), and region 1 (of cell 1 and 6) are estimated and denoted as σ_4, σ_2 and σ_1 respectively. The following two hypotheses are considered. The first one considers merging cell 4 to region 1 as follows:

$$H_0 : \sigma_4 = \sigma_1 \; vs. H_1 : \sigma_4 \neq \sigma_1 .$$

The other hypothesis considers the merging of cell 4 to the new region 2, i.e., keeping cell 4 in the region consisting of cells 2 and 3:

$$H_0 : \sigma_4 = \sigma_2 \; vs. H_1 : \sigma_4 \neq \sigma_2 .$$

If the first one has the higher likelihood ratio test statistics, cell 4 is split from region 2 and merged into region 1. Otherwise, cell 4 remains in region 2. The cycling phenomenon may occur. For example, cell 4 may be split from region 2 in one time and merged back into region 2 in another time. We will record the number of times that cell 4 is merged into region 2. If cell 4 is merged into region 2 for the second time, then cell 4 will be kept at region 2 thereafter in our current approach.

2.3. Stepwise Merging/Splitting

There are a variety of possible merging and splitting for all the initial cells generated

by the watershed transform. In order to decide which merging and splitting shall be preformed first, we use stepwise merging/splitting. That is, at each time, we only choose one merging/splitting among all possible cases belonging to Types Ⅰ, Ⅱ, and Ⅲ. This is selected by the maximum value of the likelihood ratio test statistics by exhaustive search among all possible merging/splitting of one cell.

For instance, we can use the Rayleigh distribution, as given in Eq. (1), for modeling of speckle noises in ultrasound images.

$$P(I_j \mid \sigma_i) = \frac{I_j}{\sigma_i^2} e^{\frac{-I_j^2}{2\sigma_i^2}} \tag{1}$$

the likelihood of region i is

$$P(R_i \mid \sigma_i) = \prod_{j=1}^{n_i} P(I_j \mid \sigma_i) = \prod_{j=1}^{n_i} \frac{I_j}{\sigma_i^2} e^{\frac{-I_j^2}{2\sigma_i^2}} \tag{2}$$

The maximum likelihood estimate (MLE) of σ_i of region i turns out to be

$$\hat{\sigma}_i = \sqrt{\frac{\sum_{j=1}^{n_i} I_j^2}{2n_i}}. \tag{3}$$

For the hypothesis testing of one cell, R_i, to the other cell (or region), R_j, the following likelihood ratio test is used. The number of pixels in R_i and R_j are denoted as n_i and n_j. The estimated parameters are assumed to be σ_i and σ_j. The null and alternative hypotheses are $H_0 : \sigma_i = \sigma_j = \sigma$ *vs.* $H_1 : \sigma_i \neq \sigma_j$. Under H_0, the likelihood becomes

$$\begin{aligned} L(\sigma \mid R_i, R_j) &= P(R_i \mid \sigma) P(R_j \mid \sigma)) \\ &= \prod_{k=1}^{n_i} P(I_k \mid \sigma) \prod_{l=1}^{n_j} P(I_l \mid \sigma) \\ &= \sigma^{-2(n_i+n_j)} \exp\{-\frac{\sum_{k=1}^{n_i} I_k^2 + \sum_{l=1}^{n_j} I_l^2}{2\sigma^2}\} \prod_{k=1}^{n_i} I_k \prod_{l=1}^{n_j} I_l. \end{aligned} \tag{4}$$

The MLE of σ under H_0 turns out to be

$$\hat{\sigma} = \sqrt{\frac{\sum_{k=1}^{n_i} I_k^2 + \sum_{l=1}^{n_j} I_l^2}{2(n_i + n_j)}} \tag{5}$$

Under H_1, the likelihood is

$$\begin{aligned} L(\sigma_i, \sigma_j \mid R_i, R_j) &= P(R_i \mid \sigma_i) P(R_j \mid \sigma_j) \\ &= \prod_{k=1}^{n_i} P(I_k \mid \sigma_i) \prod_{l=1}^{n_j} P(I_l \mid \sigma_j) \\ &= \sigma_i^{-2n_i} \sigma_j^{-2n_j} \exp\{-(\frac{\sum_{k=1}^{n_i} I_k^2}{2\sigma_i^2} + \frac{\sum_{l=1}^{n_j} I_l^2}{2\sigma_j^2})\} \prod_{k=1}^{n_i} I_k \prod_{l=1}^{n_j} I_l \end{aligned} \tag{6}$$

The MLE of σ_i becomes

$$\hat{\sigma}_p = \sqrt{\frac{\sum_{k=1}^{n_p} I_k^2}{2n_p}}. \tag{7}$$

Therefore, the likelihood ratio test statistic is

$$\begin{aligned} \lambda(R_i, R_j) &= \frac{L(\hat{\sigma} \mid R_i, R_j)}{L(\hat{\sigma}_i, \hat{\sigma}_j \mid R_i, R_j)} \\ &= (\frac{\hat{\sigma}_i}{\hat{\sigma}})^{2n_i} (\frac{\hat{\sigma}_j}{\hat{\sigma}})^{2nj} \exp\{\frac{(\hat{\sigma}^2 - \hat{\sigma}_i^2) \sum_{k=1}^{n_i} I_k^2}{2\hat{\sigma}^2 \hat{\sigma}_i^2} + \frac{(\hat{\sigma}^2 - \hat{\sigma}_j^2) \sum_{l=1}^{n_j} I_l^2}{2\hat{\sigma}^2 \hat{\sigma}_j^2}\}. \end{aligned} \tag{8}$$

The larger the ratio is, the more likely these two cells (or regions) shall be merged. Therefore, we will compute the likelihood ratio test statistics for all possible cases and select that one has the largest value to merge and split.

After this iterative procedure completes, all cells will be merged into different regions. Then, these regions will be regarded as new cells and further merging/splitting process can repeat. This kind of repetition will stop when the largest value of likelihood ratio test statistics is smaller than a predefined threshold.

3. Feature Extraction and Classification

At least two types of sonographic features have been used clinically in differentiating hemangiomas from HCC. One is the regional information inside and outside the tumors. The other is the local property in the vicinity of the tumor boundary such as halo. Since the local information around the boundary demands a more sophisticated characterization, in this pilot study, we have first examined the differentiation power of the regional information.

Co-occurrence matrix is one of the most widely used approaches for characterization of the sonographic textures. In this study, we have considered four co-occurrence matrix based features, namely, contrast (CON), correlation (COR), entropy (ENT),

and angular second moment (ASM), which are defined below.

Contrast

$$CON = \sum_{i,j} (i-j)^2 CO(i,j)$$

Correlation

$$COR = \frac{\sum_{i,j} ijCO(i,j) - m_x \cdot m_y}{S_x \cdot S_y}$$

where

$$m_x = \sum_i i \sum_j CO(i,j)$$

$$m_y = \sum_j j \sum_i CO(i,j)$$

$$S_x^2 = \sum_i i^2 \sum_j CO(i,j) - m_x^2$$

$$S_y^2 = \sum_j j^2 \sum_i CO(i,j) - m_y^2$$

Angular Second Moment

$$ASM = \sum_{i,j} [CO(i,j)]^2$$

Entropy

$$ENT = -\sum_{i,j} CO(i,j) \log CO(i,j)$$

where $CO(i,j)$ denotes the co-occurrence matrix element (i,j), which counts the number of pixel pairs simultaneously satisfying the following two conditions. One is that the distance and the azimuth angle between these two pixels are (d,θ), respectively, as defined in advance. The other is that the gray level of one pixel is *i* and that of the other is *j*. Twenty-four combinations of (d,θ) have been taken into account in this study to account for the complex sonographic texture pattern. They are $\{(d,\theta) \mid d = 1\text{K } 6, \theta = 0^\circ, 45^\circ, 90^\circ, 135^\circ\}$.

In addition to these four features, three features based on local means and local variances have been developed to characterize the texture and the relative brightness of the tumors. Two of these three features are the mean (μ_l) and the standard deviation (σ_l) of the means of the local 15×15 windows. The third one is the mean (μ_{vm}) of the ratio of the variance-to-means of the local 15×15 windows.

Since the gray levels and the textures may vary with the setting of the ultrasound imaging systems, the aforementioned features may be setting-dependent. To minimize the setting dependency, in this study, instead of using these features directly, we compute these features for both of the tumor area and the non-tumor area within the ROI of each image. The final quantity of each feature used for classification is the ratio of the feature value from the tumor area to that from the non-tumor area.

The total number of ratio features under considerations is 99. To avoid the curse of dimensionality [5], feature selection has been performed based on the forward sequential search approach [6] using the logistic discrimination function [7]. The selected features are then fed into the classifier, which is a multi-layer feed-forward neural network (MFNN). Performance evaluation for both feature selection and classification are based on leave-one-out cross-validation.

4. Experimental Results and Discussions

Figs. 2 and 3 show the performance of the cell-based region competition algorithm for the hypo-echoic and hyper-echoic hepatic tumors. For both of Figs. 2 and 3, the left image shows the initial cells derived by using the watershed transform and the right one shows the segmentation results attained by the proposed cell-based region competition algorithm. It is clear that the tumors in both images have been successfully delineated. At the same time, regions with significant boundaries with their adjacent areas have also been identified.

To evaluate the performance of the proposed features and classification scheme, 80 HCCs and 85 hemangiomas have been collected from the NTU hospital. Seven ratio features have been selected in most cases, including $ENT(2,0^\circ)$, $COR(2,90^\circ)$, $COR(1,45^0)$, $ASM(1,135^\circ)$, μ_l, σ_l, and μ_{vm}. The accuracy, sensitivity and specificity derived based on leave-one-out cross-validation are 83.64%, 88.75% and 78.82%, respectively. The performance is

just fine given the condition that only the regional information has been used. It is expected that the performance can be further improved by incorporating the local information in the vicinity of the boundary.

5. Conclusions

At the end of this three-year project, several segmentation schemes have been proposed to detect the tumor boundaries in an ultrasound image with either a single tumor or multiple ones. In this year, we have developed a new segmentation scheme for identifying multiple objects at the same time. Moreover, we have designed a classifier with seven regional ratio features, including four co-occurrence based and three variance-to-mean based ratio features. The promising performance indicates that it is possible to attain a clinically useful CAD system by further incorporating the local property in the vicinity of the boundary.

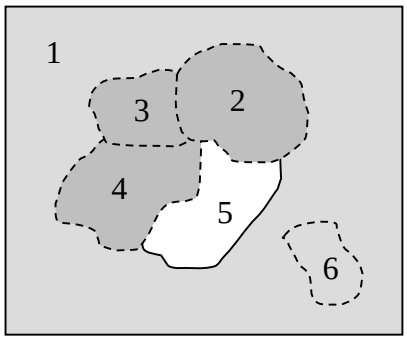

Figure 1. Cell 4 is split from region 2 (the light gray area) and merged into region 1 (the dark gray area).

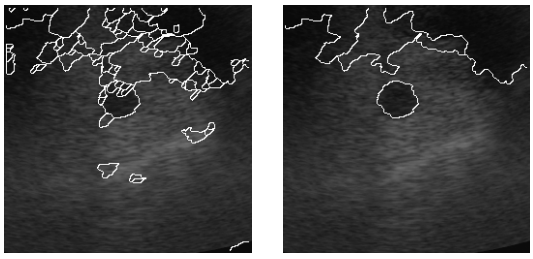

Figure 2. Performance for a hypo-echoic hepatic tumor. The left image shows the initial cells derived by watershed transform, and the right image is the segmentation result by the proposed cell-based region competition.

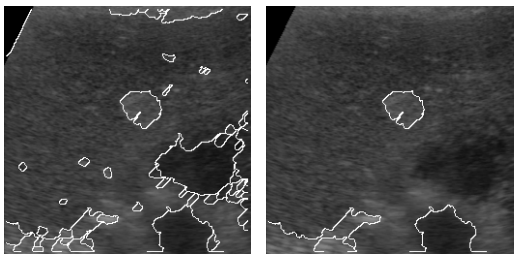

Figure 3. Performance for a hyper-echoic hepatic tumor. The left image shows the initial cells derived by watershed transform, and the right image is the segmentation result by the proposed cell-based region competition.

6. References

[1] L. Vincent and P. Soille. "Watersheds in digital spaces: an efficient algorithm based on immersion simulation," *IEEE Trans. PAMI*, 13:583-597, 1991.

[2] K. Haris, S. N. Efstratiadis, N. Maglaveras, A. K. Katsaggelos, "Hybrid image segmentation using watersheds and fast region merging," *IEEE Trans. Image Processing*, 7: 1684-1699, 1998.

[3] J. M. Gauch, "Image segmentation and analysis via multiscale gradient watershed hierarchies," *IEEE Trans. Image Processing*, 8: 69-79, 1999.

[4] S. C. Zhu and A. Yuille, "Region competition: unifying snakes, region growing, and Bayes/MDL for multiband image segmentation," IEEE Trans. PAMI, 18: 884-900, 1996.

[5] V. Cherkassky and F. Mulier Learning from data: concepts, theory, and methods. New York: John Wiley & Sons, 1998.

[6] D. C. He, L. Wang, and J. Guibert, "Texture discrimination based on an optimal utilization of texture features," Pattern Recognition 1989; 21: 141-146.

[7] W. R. Dillon and M. Goldstein, Multivariate analysis: method and applications. New York: John Wiley & Sons, 1984.